

a-Si:H/a-Si:H stacked cell from VHF-deposition in a single chamber reactor with 9% stabilized efficiency

R. Platz, D. Fischer, S. Dubail and A. Shah

Institut de Microtechnique, Université de Neuchâtel
Rue A.-L. Breguet 2, CH-2000 Neuchâtel

Abstract

In the present paper we present results on a-Si:H/a-Si:H stacked cells deposited in a single chamber reactor by the very high frequency - glow discharge (VHF-GD) deposition technique at 70 MHz. Hydrogen dilution of the i-layer yields more stable amorphous p-i-n solar cells, similar to what is observed for RF deposition. High dilution ratios of the i-layer are found to enhance contaminations. This is, for the single chamber reactor, due to the etching effect of the highly reactive H₂-plasma. Additionally, oxygen incorporation into the i-layer is favored by the high hydrogen dilution. Different means to suppress these contaminations are employed and discussed. Regarding the stacked cell design, we show by experiment and simulation that it is important to carefully adjust the current mismatch between the component cells such as to obtain a slight top-cell-limited behavior after degradation. We present an a-Si:H/a-Si:H stacked cell with an initial efficiency of 9.8 % showing only 8 % relative degradation which results in a stabilized efficiency of 9 %. The deposition rate of the employed H₂-diluted i-layer material is 4 Å/s. It is therefore demonstrated that it is possible to make highly efficient stacked cells showing good stability also in a single chamber system and employing the VHF technique to obtain higher rates.

Introduction

Very encouraging results for stabilized solar cell efficiencies have been achieved at different laboratories, all of them using multichamber reactors for the deposition of a-Si:H based solar cells: triple junction: USSC 11.8% [1]; double junction: Sanyo 10.6% [2], Solarex 9.6% [3], Fuji 10% [4], PST 6.3% for a 0.6 m² commercial module [5], Research Center Jülich 9.2% [6]). In References [1-3], a-SiGe:H alloys are employed for the middle and/or bottom cells, references [4-6] do not use a-SiGe:H alloys. Today, most solar cells are deposited in a multichamber reactor, at least in the case of industrial production. However, still a number of industries (e.g. NAPS France [7], APS [8], Solems [9]) deposit cells in a single chamber system, as such a system can be an economically interesting alternative to expensive multichamber systems.

When employing hydrogen (H₂) dilution for the deposition of more stable i-layers [10], contamination of the i-layer with oxygen, but also boron and phosphorus, can become a major problem. Oxygen contamination is probably to some extent a problem for all deposition systems whereas cross-contaminations of the dopant gases may not play such an important role in the case of multichamber systems.

The VHF deposition technique at 70 MHz has shown to yield much higher growth rates than for "standard" 13.56 MHz deposition [11], which becomes even more interesting in the case of H₂-dilution of the i-layer where deposition rates generally strongly decrease. However, there have still been questions persisting whether cells obtained from VHF deposition at higher growth rates would be less stable than

"slowly" grown cells from "conventional" RF deposition at 13.56 MHz. In fact, for RF deposition, an increase in deposition rate is found to be harmful for the stability of the solar cells [12,13,14,15,16].

In the present paper, the authors present an a-Si:H/a-Si:H stacked cell deposited in a single chamber reactor with the VHF deposition technique which has 9% stabilized efficiency and a relative degradation of only 8%. The i-layer of this cell has been deposited at a rate of 4 Å/s. A part from presenting in detail this result, the present paper will also treat systematically the problem of oxygen, phosphorus and boron contamination in the context of the fabrication of p-i-n cells based on VHF plasma deposition with H₂-dilution, furthermore the delicate question of optimizing the stabilized efficiency of a stacked cell.

I. Experimental

All samples (i-layers and complete p-i-n or stacked solar cells) were deposited in a single chamber reactor with load lock using the very high frequency - glow discharge technique (VHF-GD) at 70 MHz. The RF input power of about 30 mW/cm² is coupled capacitively to the plasma. Substrate size is 8x8 cm², the electrode distance is 1.6 cm. Intrinsic layers were deposited on glass substrates (AF45, Schott) and crystalline silicon wafers for infrared absorption measurements. The optical gap E₀₄ ($\alpha(E_{04}) = 10^4 \text{ cm}^{-1}$) was determined from transmission and reflection measurements using a Perkin Elmer Lambda 900 spectrometer. Infrared spectra measurements were performed using a Perkin Elmer FT-IR 1720X spectrometer. All cells are made on Asahi U-type TCO (SnO₂). We use silane (SiH₄), methane (CH₄) and diborane (B₂H₆) for the amorphous p-layer. The i-layers are made from SiH₄ with or without hydrogen (H₂) dilution. For the n-layers we employ PH₃, SiH₄ and H₂. These layers are partly amorphous, partly microcrystalline. A detailed description of the n-layer can be found in [17]. We use sputtered ZnO or ITO together with silver as back contact. Anti reflecting coatings on the front-side of the cells have not been employed. Solar cells are measured at 25°C using a double source Solar Simulator (Wacom WXS-140S). Spectral response measurements are performed at varying bias voltages using a probe beam spot smaller than the cell surface. Integration of the measured curve is used to control the cell current independently of the effective cell surface. Degradation experiments were performed at 50°C under open circuit conditions using photoluminescence tubes with a near-daylight spectrum as light sources.

II. Optimizing the single cell

2.1. Hydrogen dilution

We deposited 2 series of cells (at substrate temperature T_S=220°C and T_S=180°C) containing i-layers of 450 nm thickness deposited at different H₂-dilution ratios ($=[\text{H}_2]/[\text{SiH}_4]$). These series of cells were systematically degraded for 1000 h at 50°C under white light (1 sun intensity) and open circuit conditions. The E₀₄ values of the corresponding intrinsic layers are shown in Fig.1. Additionally, we show in this figure the values for i-layers deposited at T_S=150°C. For a constant deposition temperature we observe an increase of the optical gap E₀₄ with hydrogen dilution. When comparing H₂-dilution ratios to the values of other laboratories one must take care of the fact that the H₂-concentration in the plasma depends on the pumping system; we employ a Roots pump for pumping the process gases during deposition. Due to the VHF deposition technique, we are limited towards high dilution ratios by the early onset of microcrystalline growth which appears for VHF-GD (70 MHz) at a dilution ratio of approximately 13 [18].

Fig.2a-d. show the V_{OC} , FF, I_{SC} and efficiency values for these cells in the initial (black symbols) as well as in the degraded state (open symbols). The increase in the optical gap is reflected in the V_{OC} values for these cells which also increase with increasing H_2 -dilution; furthermore, an increase in the optical gap due to reduction of the deposition temperature leads also to an increase of the V_{OC} . The V_{OC} -values remain almost stable during degradation, in contrast to cells with an a-SiC:H buffer layer [19]; for the 220°C samples and for high dilution ratios at 180°C we even find an increase of the V_{OC} during degradation. Hydrogen dilution improves the fill factor after degradation for the cells deposited at 180°C. For the 220°C cells, the degraded fill factor is only slightly improved by H_2 -dilution. However, for both temperatures, current degradation is strongly reduced by H_2 -dilution (Fig.2b.). The gain in V_{OC} and the better stability of the fill factor value is to some extent counteracted by a loss in the optical absorption due to an increase of the optical gap under H_2 -dilution as shown in Fig.1. For the 220°C samples, the higher V_{OC} is compensated by a lower current, whereas for the 180°C samples the gain in V_{OC} and FF after degradation is larger than the loss in current. For dilution ratios of 2 and higher, both series have the same efficiency in the degraded state, one cell having a higher current and smaller V_{OC} , the other cell the inverse. This possibility of a choice between current and voltage is particularly interesting in the context of tandem and stacked cell optimization.

Fig.3. shows the deposition rates for different dilution ratios at $T_S=180^\circ\text{C}$. The deposition rate decreases approximately linearly with dilution, starting from the already rather high value of 4.5 Å/s at 4 W (30 mW/cm²) input power. The power values given here have not been corrected for network losses, the given values are those directly measured between the generator and the matching network. At a dilution ratio of 9 we still obtain a deposition rate of over 2 Å/s. The input power of 4 W has been chosen arbitrarily, it is possible to deposit material at higher rates by increasing the input power as shown in Fig.3. There is no difference in degradation in between cells incorporating the 4 W or the 8 W material. Especially at high H_2 -dilution ratios, the decrease of deposition rate can become a problem for efficient industrial production. There is very few data about deposition rates available in the literature, however generally RF deposition without dilution yields deposition rates in the order of 1-2 Å/s [14,15,20,21]. Deposition rates for diluted i-layers may reach 2 Å/s [22] for a highly optimized process, in most cases, however, values around [23] or below 1 Å/s [24,25] depending on the dilution ratio of the i-layer are reported. Microwave glow discharge yields deposition rates of up to 100 Å/s for a-SiGe:H alloys deposited with H_2 -dilution [26,27], however even at a reduced deposition rate of 10 Å/s, the degradation of such cells is still larger than for cells containing RF deposited i-layers at 1 Å/s [28].

2.2. Contaminations

While optimizing our cells, various contamination problems had to be addressed. These problems can be divided into two groups: The first group are problems due to the single chamber system, i.e. mainly cross-contamination by the dopant gases; the second group are problems which can also appear in multichamber systems. In this second group, we have to deal mainly with oxygen originating from different sources. We found both groups of problems to become much more important when depositing i-layers under H_2 -dilution.

2.2.1. Oxygen

Incorporating a series of i-layers with different dilution ratios into thick (450 nm) solar cells, we observed a decrease of the fill factor with increasing dilution ratio (Fig.4., lower curve). This decrease in the fill factor is due to a strongly voltage-dependent spectral response (SR) in the red wavelength (650 nm) region (Fig.4., upper curve). For a dilution ratio of 9 we could increase the fill factor by doubling the deposition power, thereby increasing the deposition rate.

We attribute this decrease in the FF to the n-doping effect of the oxygen contamination [29]. It has already been shown by Kroll et al. [30] that H₂-dilution can increase the oxygen incorporation in amorphous layers. In general, less oxygen is incorporated at higher growth rates due to e.g. an increased plasma power. One source of oxygen contaminations is the outgassing rate of the reactor, i.e. H₂O coming from the chamber walls. This outgassing rate is influenced e.g. by the temperature of the chamber walls. Fig.5. shows V_{OC} and the parameter $FF^* = FF \cdot I_{SC} / I(-3V)$ for 450 nm thick cells deposited under different outgassing conditions and a H₂-dilution ratio of 9. The parameter FF* is used here because for thick cells and in the presence of significant contaminations the current may not yet be saturated at 0V. Filled symbols indicate the initial values. The decrease of FF* with increasing outgassing rate is quite evident, whereas the V_{OC} values remain nearly unchanged. It is noteworthy that the relative degradation of the strongly oxygen-contaminated cells is not stronger than that of the cells with an uncontaminated i-layer. The experiment shows that the reactor outgassing rate is much more important when depositing with strong H₂-dilution ratios than for the case of undiluted i-layers where we have indeed never observed a dependence of the FF on the outgassing rate.

Having reduced the outgassing rate of the reactor to a large extent by heating the chamber walls overnight and cooling down before deposition, a part of the oxygen problem still remains. We attribute the remaining contamination to impurities in the feedstock gases and employed a gas-purifier [30]. Thereby the decrease in the red spectral response could be further reduced. Fig.6. shows the collection efficiency ($=SR(0V)/SR(-3V)$) of 3 450 nm thick solar cells. Curve "1" corresponds to a cell deposited without gas purifier, curve "2" is that of the same cell, where a gas purifier had been employed for the i-layer. Note that the i-layer thickness is 450 nm. For thinner cells, this effect of reduced collection is hidden behind field-enhanced collection and is observed only to a much smaller extent.

2.2.2. Phosphorus

For curve "2" (Fig.6.), the red collection efficiency is still reduced. We attribute this to phosphorus contamination of the i-layer. This should appear only in single chamber reactors. Usually, we deposited a "dummy layer" after the n-layer of the last cell which covers the electrodes and prevents from phosphorous contamination of the next cell (see Fig.9., for a single cell the process is terminated after the first n-layer). This worked very well for cells deposited from undiluted or only slightly diluted SiH₄-plasma. When depositing the i-layer from a highly diluted plasma we again obtained an n-doping effect in the i-layer. The strongly reactive H₂-plasma reaches uncovered parts of the reactor or parts which had been covered only with a thin dummy layer and etches the material containing phosphorus which afterwards is incorporated into the i-layer. Conclusively we made the dummy layer also with a strongly diluted SiH₄-plasma at the very low pressure of 0.2 mbar. In this case the plasma is burning also outside the electrodes and covers all parts which can be reached afterwards by the i-layer-plasma. Thereby we obtained a further reduction of the

collection losses in the red wavelength region as indicated by curve "3" in Fig.6. and a fill factor for the 450 nm thick cell of 70 %.

2.2.3. Boron

From Fig.6. one can further see that the collection of blue light is reduced as soon as the strong oxygen-contamination is taken away. This is obviously due to boron contamination which is then no more compensated by oxygen. Boron contamination appears mainly in the case of single chamber reactors. However, also for multi-chamber systems, contamination from the substrate holder is sometimes discussed. After the deposition of the p-layer we take the substrate out of the chamber into the loadlock. A CO₂-plasma at relatively high pressure (1 mbar) and high power efficiently removes boron from the chamber [31] when the i-layer is deposited without dilution or with only small H₂-dilution ratios. However, when a strong H₂-dilution is employed for the successive i-layer deposition, we find boron contamination in the i-layer which is detected by a decreased collection for blue light as determined from spectral response measurements. If one operates the CO₂-Plasma at the same chamber pressure as the p-layer deposition (0.3 mbar), the problem is decreased to a certain amount; nevertheless there seems to be still some boron in the first part of the i-layer. We assume that this could be due to an etching of the p-layer during the deposition by a highly diluted i-layer plasma. An indication to support this hypothesis is that we need about 150 % of the normal p-layer thickness when employing highly diluted i-layers in order to get the maximum V_{OC}. Note that the transmission of the p-layer is not diminished hereby; this could indicate an etching of the p-layer during the first seconds of i-layer deposition. This has, to our knowledge, not yet been reported for RF (13.56 MHz) deposition, whereas for VHF deposition etching has already been observed under certain conditions [32].

2.3. Single cell with graded dilution

Having resolved the problems with contaminations, the question arised which amount of dilution is necessary w.r.t. stability and useful w.r.t. the increase in the optical gap. We found that a relatively thin layer with the highest gap (=highest dilution) at the p-i-interface is sufficient to achieve the maximum possible V_{OC}. Therefore we developed cells with a graded dilution ratio in the i-layer [19]. The first part of the i-layer of about 30 nm close to the p-i-interface was deposited with a high dilution ratio of 9 at 2 Å/s. The rest was deposited using a dilution ratio of only 2 at 4 Å/s. We could thereby combine a good i-layer stability (dilution ratio 2 of the bulk), avoid a too strong increase of the optical gap and still obtain a high V_{OC}. Fig.7a. shows the V_{OC} and FF values of such cells in the initial and degraded state for 3 different i-layer thicknesses, Fig.7b. the short circuit currents and the resulting efficiency values. After 1000h light-soaking, all cells show, independently of the cell thickness, an efficiency of about 7.5 %. The increase in current with increasing i-layer thickness is compensated by a stronger fill factor degradation.

Due to their high V_{OC}, only slightly reduced short circuit current, and excellent stability, these cells with a graded hydrogen dilution ratio have already been successfully incorporated as top cells in micromorph tandem cells [33,34].

III. Optimizing the stacked cell

3.1. General considerations

Whereas for the top cell in a tandem or stacked structure, the loss in absorption due to H₂-dilution can easily be compensated by an only slightly thicker i-layer, the situation is more difficult for the bottom cell. Its current must be large enough to at least match the current of the top cell. It has been shown that it is possible to reduce light-induced degradation by making the stacked cell top-limited [35]. The following simple simulation shows that, in fact, a stacked cell has the highest output power if its current is limited by the top-cell in the degraded state.

The simulation is based on measured I-V-curves of single junction p-i-n cells in different states of degradation. In order to estimate the I-V-curve of a stacked cell we simply added the V(I) curves of the both component cells. The current values of the component cells were scaled before in order to obtain different degrees of mismatch. The total cell current ($= I_{\text{top}} + I_{\text{bottom}}$) was held constant at 15 mA/cm². Scaling of the currents was done with respect to the value at -2 V ($I_{\text{top}}(-2\text{V}) + I_{\text{bottom}}(-2\text{V}) = 15 \text{ mA/cm}^2$) thereby taking into account I_{SC} degradation. A relatively small source of error consists in the fact that the bottom cell in a real tandem cell sees only light filtered by the top cell, i.e. only the red part of the spectrum. However, by comparing cell measurements under white and filtered red light, we found only minor differences in the I-V-curves. Based on this we contend that this simulation method describes quite well the real I-V-curve and allows us to easily model the situation for different degrees of mismatch and for different top and bottom cells.

Fig.8a. shows the dependence of the output power of the stacked cell ($= V_{\text{OC}} \cdot I_{\text{SC}} \cdot \text{FF}$) as a function of the current mismatch for different pairs of top and bottom cells. For two cells with the same fill factor, the maximum output power is obtained for matched cell currents. In a stacked cell, however, the bottom cell will always degrade to a larger extent than the thin and highly stable top cell. Thus, if we pair a high-FF top cell with a bottom cell showing a lower fill factor, we observe a shift of the point of maximum power towards slightly top-limited conditions (to the left in Fig.8a.). Reducing the difference in FF of the both cells, the maximum power is again obtained for a smaller mismatch. The model indicates that the optimum mismatch is found somewhere below a difference in current of 1 mA/cm², depending on the fill factors of both the top and the bottom cell. For realistic conditions we expect an optimum mismatch to be around 0.5 mA/cm². Fig.8b. shows the FF values for the same conditions as in Fig.8a. It is quite obvious that maximum output power is not found for maximum fill factor values which increase for increasing mismatch and are minimum around matched currents. For a high degree of mismatch, one can obtain very high FF values, however the power is low because of a small cell current. Note that Fig.8. shows extreme conditions. E.g. $I_{\text{top}} - I_{\text{bottom}} = -6 \text{ mA/cm}^2$ means 4.5 mA/cm² for the top cell and 10.5 mA/cm² for the bottom cell. Also shown in Fig.8b. are measured FF values for stacked cells in the initial and degraded state. The current value of the top (bottom) cell is determined from SR measurements applying a voltage bias corresponding to the V_{OC} of the bottom (top) cell of the stack and using a red (blue) light bias. The model fits the measured values astonishingly well.

Thus, in order to have a maximum power output after degradation, it is necessary to maintain top-limited conditions after degradation, as has been shown. The FF of the bottom cell is smaller than that of the top cell because of the large difference in thickness of the two cells. The thickness of the top cell is 50-80

nm, whereas the bottom cell thickness is around 300 nm. Furthermore, the top cell is made from strongly diluted i-material, whereas the bottom cell contains mainly undiluted material (see below). As a consequence, the top cell nearly does not degrade whereas the bottom cell suffers relatively strong degradation.

3.2. The optimized process

Fig.9. shows a flow chart of our process for the deposition of an a-Si:H/a-Si:H stacked cell. Deposition and process times are indicated in the boxes. Total process time including 20 minutes of substrate pre-heating is 98 min. Including the cleaning step after the last n-layer i.e. an intrinsic layer deposited on a stainless steel substrate, the whole cell can be made in less than 2 1/2 hours. For the deposition alone, including the i-layers, we need only 22 min.; this low value is obtained by employing the VHF deposition process. Thus, the largest part of the whole time is used here for cleaning steps in between doped and intrinsic layers; these cleaning steps are necessary because of our single chamber reactor. Schropp et al. [7] report for a stacked cell deposited also in a single chamber (but at 13.56 MHz) a deposition time of at about 130 min. without any cleaning step in between doped and intrinsic layers and without H₂-dilution for the i-layers.

3.3. Stacked cell with 9 % stabilized efficiency

Taking as a goal an initial efficiency of 10 %, one needs with a V_{OC} of 1.75 V and a fill factor of 74 % a current of 7.7 mA/cm². This means at least 8 mA/cm² for the bottom cell in the initial state in order to maintain top-limited conditions after degradation (see section 3.1.). This is not achievable with a diluted i-layer in the bottom cell and at low temperature (180°C). Therefore, we deposited the bottom cell at standard temperature (220°C) and without H₂-dilution. Again, a thin "buffer layer" of diluted material was inserted at the p-i-interface, increasing thereby the V_{OC} of the bottom cell. The top cell had to be heated up after the deposition of the n-layer during 10 min. (Fig.9.) before starting to deposit then the p-i-i-n-structure of the bottom cell; this deposition was carried out in less than 15 min. The heating of the top cell does not have any detrimental effect on the fill factor, as long as the time at high temperature is kept relatively short. The V_{OC} of the stacked cell, however, is about 50 mV smaller than for an entirely low-temperature cell and it does degrade slightly. However, by employing this technique of depositing bottom and top cells at different temperatures, the bottom cell provides enough current and still can be rather thin. The I-V-curve of such a two-temperatures p-i-i-n-p-i-i-n stacked cell is shown in Fig.10a. The initial efficiency is 9.8 %, after 300h degradation the efficiency stabilizes at 9 % (8.6±0.6 % according to the measurement by the Fraunhofer-ISE Kalibrierlabor, Freiburg / Germany) which means a relative degradation of only 8 % (Fig.10b.). Degradation is partly due to V_{OC} , the stabilized fill factor of 69 % is quite high. The cell has a current mismatch of 0.56 mA/cm² in the initial and of about 0.3 mA/cm² in the degraded state which confirms the considerations of section 3.1. that the highest stabilized power can be achieved by a slight current mismatch for component cells with different fill factors.

Conclusions

Hydrogen dilution and an appropriate design of the p-i-n cell yields solar cells with high initial and stabilized efficiencies. We have shown that in a single chamber reactor also, highly efficient solar cells can be fabricated if contaminations are counteracted by appropriate measures. Phosphorus contamination can be suppressed by a low-pressure H₂-diluted SiH₄ plasma which covers the walls and hinders phosphorus from the underlying layers to be etched. Boron is efficiently removed from the reactor by a CO₂-plasma. Here again, care has to be taken that the plasma reaches all regions of the reactor which are touched afterwards by the highly reactive H₂-diluted plasma of the following i-layer.

The VHF deposition technique at 70 MHz yields remarkably increased deposition rates as compared to conventional RF deposition. This is even more interesting for H₂-diluted layers as deposition rates generally decrease strongly with the H₂-dilution ratio. Pure deposition time for our a-Si:H/a-Si:H stacked cell including H₂-diluted layers is 22 min., the diluted i-layers being deposited at 4 Å/s.

High stabilized efficiency values can be achieved for a-Si:H/a-Si:H stacked cells if the current mismatch between the top and the bottom cell is maintained after degradation. In order to provide enough current for the bottom cell, we deposited the bottom cell at a higher temperature (220°C) than the top cell (180°C). The necessary short heating-up of the top cell before and during bottom cell deposition has no adverse effect on the top cell properties. A combination of 2 different dilution ratios in both i-layers yields a combination of high V_{OC} values, sufficient current and good stability.

We presented an a-Si:H/a-Si:H stacked cell with an initial efficiency of 9.8 % and a stabilized efficiency of 9 % which had been deposited in a single chamber using the VHF deposition technique at 70 MHz. This result is comparable to stabilized efficiencies for stacked cells not containing germanium in the bottom cell of other laboratories, but using multichamber systems and 13.56 MHz RF-deposition. It is therefore demonstrated that it is possible to make highly efficient stacked cells showing good stability also in a single chamber system and employing the VHF technique to obtain higher deposition rates.

Acknowledgments

Financial support by Swiss Federal Department of Energy BEW/OFEN, grant EF-REN (93)032 is gratefully acknowledged.

References

- 1 J. Yang, X. Xu, A. Banerjee and S. Guha, Proc. 25th IEEE PVSC (1996) to be published.
- 2 Y. Hishikawa, K. Ninomiya, E. Maruyama, S. Kuroda, A. Terakawa, K. Sayama, H. Tarui, M. Sasaki, S. Tsuda and S. Nakano, Solar Energy Materials and Solar Cells 41/42 (1996) 441.
- 3 Y.-M. Li, L. Yang, M.S. Bennett, L. Chen, F. Jackson, K. Rajan and R.R. Arya, MRS Symp. Proc. 336 (1994) 723.
- 4 Y. Ichikawa, S. Fujikake, T. Yoshida, T. Hama and H. Sakai, Proc. 21st IEEE PVSC (1990) 1475.
- 5 A. Bubenzer, P. Lechner, H. Schade and H. Rübél, Techn. Dig. PVSEC-7 (1993) 263.
- 6 B. Rech, C. Beneking, S. Wieder, T. Eickhoff and H. Wagner, Proc. 13th EC-PVSEC (1995) 613.

- 7 R.E.I. Schropp, M.B. von der Linden, J. Wallinga, D. Knoesen, J. Hyvärinen, J. Skarp, T. Suntola, J.A. Willemen, M. Zeman, J.W. Metselaar, W. Loyer, D. Guillardau, E. Fabre, Proc. 1st WCPEC (1994) 626.
- 8 J. Macneil, A.E. Delahoy, F. Kampas, E. Eser, A. Varvar and F. Ellis Jr., 21st IEEE PVSC (1990) 1501.
- 9 U. Eicker, Proc. 10th EC-PVSEC (1991) 358.
- 10 S. Guha, K.L. Narasimhan and S.M. Pietruszko, J. Appl. Phys. 52 (1981) 859.
- 11 H. Curtins, N. Wyrsh, M. Favre and A.V. Shah, Plasma Chemistry and Plasma Processing 7 (1987) 267.
- 12 S. Guha, J. Yang, S.J. Jones, Y. Chen and D.L. Williamson, Appl. Phys. Lett. 61 (1992) 1444.
- 13 X. Xu, J. Yang and S. Guha, MRS Symp. Proc. 297 (1993) 649.
- 14 P. Lechner, H. Rübel and N. Kniffler, Proc. 10th EC-PVSEC (1991) 354.
- 15 H. Schade, P. Lechner and H. Rübel, Proc. 12th EC PVSEC (1994) 89.
- 16 R.E.I. Schropp, A. Sluiter, M.B. von der Linden and J.D. Ouwens, J. Non-Cryst. Solids 164-166 (1993) 709.
- 17 N. Pellaton Vaucher, B. Rech, D. Fischer, S. Dubail, M. Goetz, H. Keppner, C. Beneking, O. Hadjadj, V. Shklover, A. Shah, to be presented at PVSEC-9, Miyazaki.
- 18 K. Prasad, thesis, Université de Neuchâtel, 1991.
- 19 R. Platz, D. Fischer, C. Hof, S. Dubail, J. Meier, U. Kroll and A. Shah, MRS Symp. Proc. 420 (1996) to be published.
- 20 M. Nishikuni, T. Takahama, S. Okamoto, K. Ninomiya, H. Nishiwaki, S. Tsuda, A. Takeoka, M. Ohnishi, S. Nakano and Y. Kuwano, Progress in Photovoltaics 2 (1994) 211.
- 21 J. Dutta, Z.Y. Wu, T. Emeraud, E. Turlot, E. Cornil, J.P.M. Schmitt and A. Ricaud, Proc. 11th EC-PVSEC (1992) 545.
- 22 S. Guha, Proc. 25th IEEE PVSC (1996) to be published.
- 23 J. Bezemer, W.G.J.H.M. van Sark, M.B. von der Linden, W.F. van der Weg, P.M. Meijer, J.D.P. Passchier and W.J. Goedheer, Proc. 12th EC-PVSEC (1994) 327.
- 24 S. Wieder, B. Rech, C. Beneking, F. Siebke, W. Reetz and H. Wagner, Proc. 13th EC-PVSEC (1995) 234.
- 25 E. Maruyama, Y. Hishikawa, M. Tanaka, S. Kiyama and S. Tsuda, MRS Symp. Proc. 420 (1996) to be published.
- 26 S. Guha, X. Xu, J. Yang and A. Banerjee, Appl. Phys. Lett. 66 (1995) 595.
- 27 K. Saito, M. Sano, K. Ogawa and I. Kajita, J. Non-Cryst. Solids 164-166 (1993) 689.
- 28 S. Suyiyama, X. Xu, J. Yang and S. Guha, MRS Symp. Proc. 420 (1996) to be published.
- 29 M. Isomura, T. Kinoshita, Y. Hishikawa and S. Tsuda, Appl. Phys. Lett. 65 (1994) 2329.
- 30 U. Kroll, J. Meier, H. Keppner, A. Shah, S.D. Littlewood, I.E. Kelly and P. Giannoulès, J. Vac. Sci. Technol. A 13 (1995) 2742.
- 31 M. Kubon, N. Schultz, M. Kolter, C. Beneking and H. Wagner, Proc. 12th EC-PVSEC (1994) 1268.
- 32 M. Heintze, W. Westlake and P.V. Santos, J. Non-Cryst. Solids 164-166 (1993) 985.

- 33 J. Meier, P. Torres, R. Platz, S. Dubail, U. Kroll, J.A. Anna Selvan, N. Pellaton Vaucher, C. Hof, D. Fischer, H. Keppner, A. Shah, K.-D. Ufert, P. Giannoulès, J. Köhler, MRS Symp. Proc. 420 (1996) to be published.
- 34 J. Meier, P. Torres, R. Platz, S. Dubail, U. Kroll, J.A. Anna Selvan, N. Pellaton Vaucher, C. Hof, D. Fischer, H. Keppner, A. Shah, K.-D. Ufert, to be presented at PVSEC-9, Miyazaki.
- 35 X. Xu, J.C. Yang and S. Guha, 23rd IEEE PVSC (1993) 971.

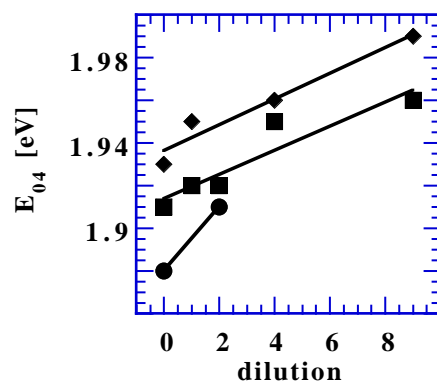


Fig.1.: E_{04} values for 150°C (◆), 180°C (■) and 220°C (●) substrate temperature and different dilution ratios. dilution = $[H_2]/[SiH_4]$.

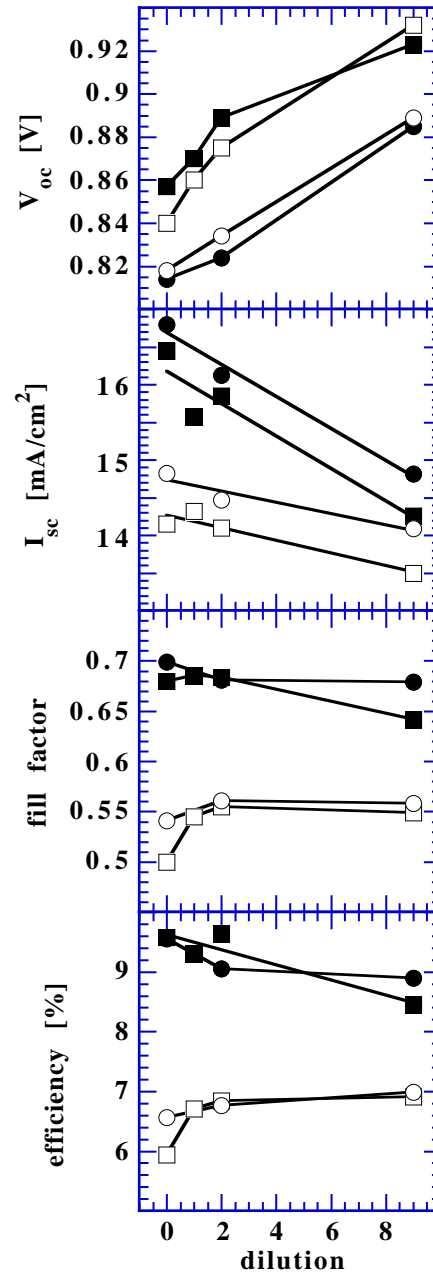


Fig.2a.: V_{oc} values for 220° and 180°C and different dilution rates before and after degradation. i-layer thickness is 450nm. ●: 220°C, ■: 180°C, black symbols before degradation and open symbols after degradation (1000h).

Fig.2b.: I_{sc} values for the same samples.

Fig.2c.: Fill factor values for the same samples.

Fig.2d.: Efficiency values for the same samples.

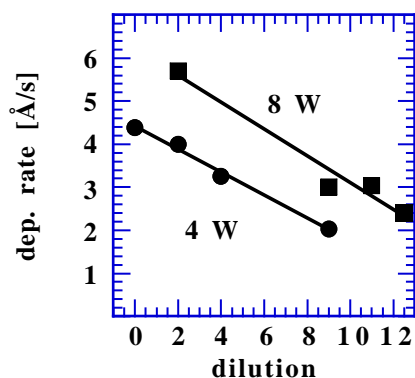


Fig.3.: Deposition rate for $T_S=180^\circ\text{C}$ and different H_2 -dilution ratios.

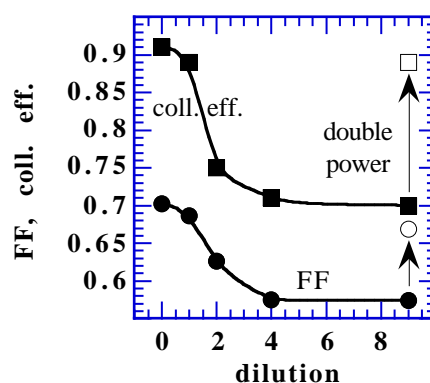


Fig.4.: Dilution series for $T_S=180^\circ\text{C}$ and 450 nm thick cells. Shown are the FF (lower curve) and collection efficiency ($=\text{SR}(0\text{V})/\text{SR}(-3\text{V})$) @ 650nm (upper curve).

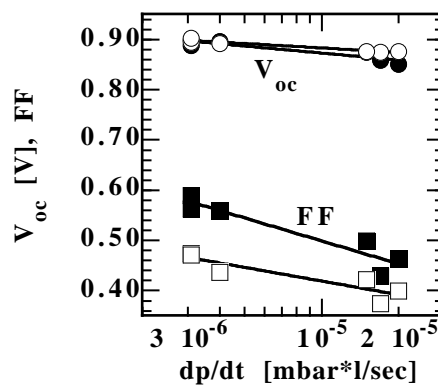


Fig.5.: V_{oc} (●) and FF (■) before (black symbols) and after degradation (open symbols) for 450 nm thick cells as a function of the reactor outgassing rate. Substrate temperature was 180°C , i-layers are deposited with a dilution ratio of 9.

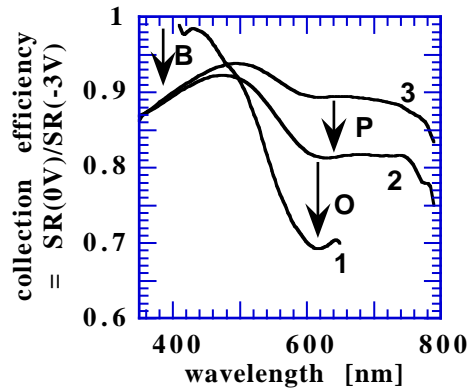


Fig.6.: Effect of different contaminations on the collection efficiency of a 450 nm thick p-i-n solar cell. Substrate temperature was 180°C, the i-layer was deposited with a dilution ratio of 9.

Curve 1: Using an undiluted dummy layer after n-deposition and CO₂-plasma at 1 mbar. Curve 2: Additionally, a gas purifier was used eliminating a large part of the oxygen contamination. Curve 3: The dummy layer after n-deposition was made using a strong H₂-dilution and low chamber pressure (0.2 mbar).

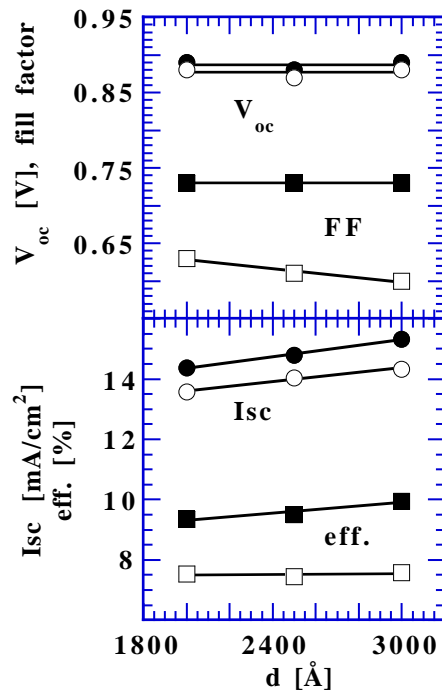


Fig.7a.: V_{OC} and FF in the initial (black symbols) and degraded (1000 h, open symbols) state for cells with graded-dilution i-layers and different i-layer thicknesses. $T_S = 180^\circ\text{C}$.

Fig.7b.: I_{SC} and efficiency in the initial and degraded (1000 h) state for the cells of Fig.7a.

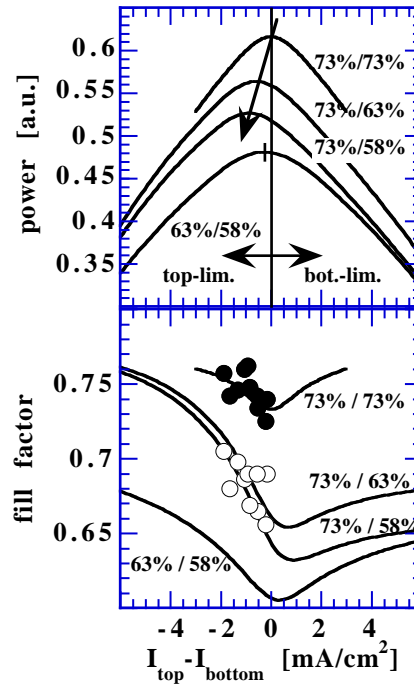


Fig.8.: Simulated output power (a) and fill factor (b) values for a-Si:H/a-Si:H stacked cells as a function of the "mismatch", i.e. of the difference in current density between top and bottom cell. The total cell current density $I_{top}+I_{bottom}$ was held constant at $15 \text{ mA}/\text{cm}^2$. Percentage values next to the curves mean fill factors of the top/bottom cell. E.g. 73%/58% means 73% FF for the top cell and 58% FF for the bottom cell. Also shown are experimental fill factor values in the initial (black symbols) and degraded (1000h, open symbols) state for a set of 10 a-Si:H/a-Si:H stacked cells deposited at $T_S = 180^\circ\text{C}/220^\circ\text{C}$ for the top/bottom cell.

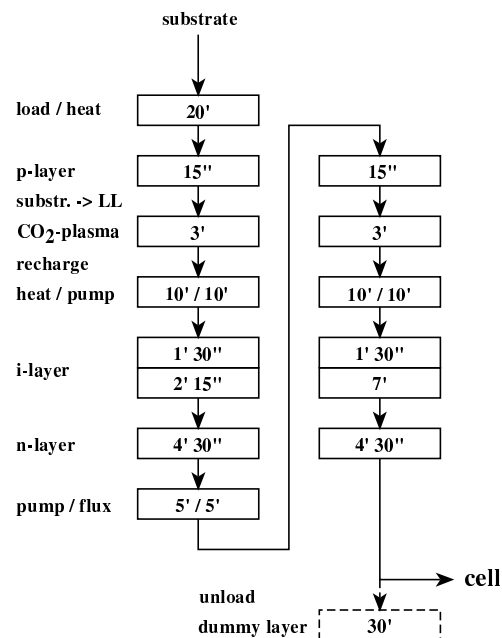


Fig.9.: Flow chart of a-Si:H/a-Si:H stacked cell deposition. Total process time is 1 h 38 min. without dummy layer deposition.

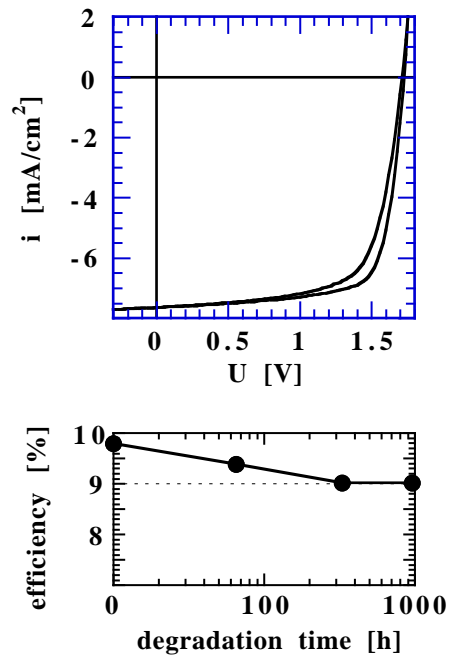


Fig.10a.: I-V-curve of an a-Si:H/a-Si:H stacked cell with a stabilized efficiency of 9 %.

initial: 1.73 V 74 % FF 7.65 mA/cm² 9.8 %.

1000h: 1.71 V 69 % FF 7.64 mA/cm² 9.0 %.

Fig.10b.: Degradation kinetics of the cell shown in Fig.10a. Saturation appears after 300h of light-soaking at 50°C under open-circuit conditions.